Preprints of the 21st IFAC World Congress (Virtual)
Berlin, Germany, July 12-17, 2020

An iterative learning approach to economic model predictive control for an integrated solar thermal system ⋆

Jacob Morrison * **Ryozo Nagamune** * **Vladimir Grebenyuk** **

* *University of British Columbia, Vancouver, BC V6T 1Z4, Canada (e-mails: jacob.morrison@ubc.ca, nagamune@mech.ubc.ca).*
** *Ascent Systems Technologies, Vancouver, BC, Canada, (e-mail: vgreb@ascentsystems.ca)*

Abstract: An iterative learning (IL) approach to disturbance prediction for economic model predictive control (EMPC) is proposed and applied to an integrated solar thermal system (ISTS). The disturbance in the system, which is the user hot water demand, is predicted iteratively by taking advantage of the repetitive nature of hot water consumption and utilized by EMPC for improved ISTS control performance. Various user load scenarios are developed for simulations based on historical data, and the performance of the proposed control method is compared against an idealistic EMPC scheme with perfect load information along with existing EMPC methods and a baseline proportional-integral controller. It is demonstrated that the proposed IL approach to EMPC achieves electrical costs within 0.5% of the idealistic case while outperforming all other methods in both energy savings and output temperature management.

Keywords: iterative learning, economic model predictive control, disturbance prediction, solar thermal energy, sustainable energy

1. INTRODUCTION

A majority of the world relies on fossil fuels to meet energy demands. These resources are harmful to the environment and do not replenish themselves, causing energy prices to rise as they become more scarce (Mohtasham, 2015). One abundantly available renewable alternative is the sun, which provides the earth with more energy in one hour than humans consume annually (Crabtree and Lewis, 2007). When it comes to solar energy, solar thermal systems are the most efficient option and are typically used for heating applications as opposed to electricity production. While heating is not the only energy requirement for humans, it represents a crucial area of need. This need is particularly strong in northern countries, where hot water accounts for approximately 25% of domestic energy consumption (Aguilar, White and Ryan, 2005).

Most solar thermal systems feature an auxiliary heat source to ensure hot water demands can be met. The combination of this external source with a solar thermal collector is called an *integrated solar thermal system (ISTS)*. When it comes to controlling an ISTS, it is important to maximize efficiency by using the auxiliary heat source intelligently. Past research into this application has found model predictive control (MPC) to be the most effective control algorithm as it can be optimized while accounting for case specific factors such as input constraints. Godina et al. highlighted the benefits of MPC by comparing its performance with on/off and proportional-integral-derivative (PID) controllers for domestic energy management (Godina et al., 2018). Weeratunge et al. then provided more insight by using MPC to reduce the operational costs of a solar assisted heat pump system compared to conventional methods (Weeratunge et al., 2018).

An issue with the majority of research to date into MPC for solar thermal and general energy saving applications, however, is the lack of consideration for the impact of different user load scenarios. Most works assume a constant daily hot water demand profile for simplicity (Edwards, Beausoleil-Morrison and Laperrière, 2015), whereas in reality user load can vary drastically, both day-to-day within a household and between different households (Armstrong et al., 2009). This is an area of concern as MPC algorithms tend to behave poorly when system output predictions are inaccurate, which would be the case with any model that assumes a single load trajectory (Ma et al., 2012).

In the past, multiple tactics have been used to predict future disturbance, such as integrated moving average models (Box et al., 2015) and artificial neural networks (Fuentes, Arce and Salom, 2018). The problems with these methods for this ISTS application are that they fail to account for cyclic day-to-day patterns and cannot learn on the go from a specific household. While different households use different amounts of hot water and this usage can vary day-to-day, these individual households tend to follow repetitive load profile patterns for a given day of the week (Energy Saving Trust, 2008, George, Pearre and Swan, 2015). With this property in mind, a more effective approach for the ISTS application is to

⋆ This work was supported by the Collaborative Research and Development Grant from the Natural Sciences and Engineering Research Council of Canada and Ascent Systems Technologies

Copyright lies with the authors

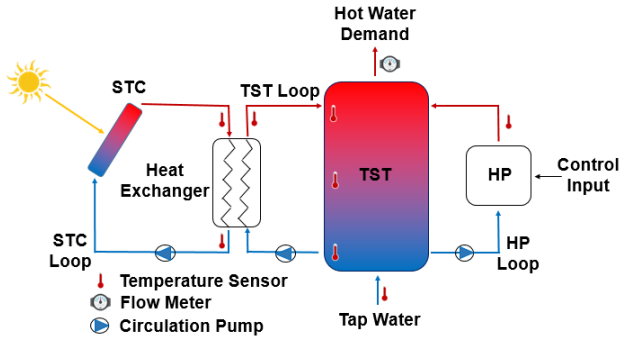

Fig. 1. Integrated solar thermal system configuration

utilize iterative learning (IL) techniques to take advantage of the repetitive nature of domestic hot water usage.

IL is based on the idea that the performance of a system completing a repetitive task can be improved by learning from past iterations of the task (Bristow, Tharayil and Alleyne, 2006). To date some attempts to combine IL with MPC have been undertaken in literature. These efforts have mainly focused on using IL to update the terminal constraints in the MPC algorithm (Rosolia and Borrelli, 2018), or to improve controller performance in batch processes by iteratively updating the model parameters or state estimation (Lee et al., 2004, Lu, Chen and Xie, 2018). In contrast, the idea presented in this paper is to use the IL framework to predict future disturbances, allowing for more efficient control.

The paper is organized as follows. In Section 2 the control problem is formulated, including a description of the ISTS to be considered. Section 3 then focuses on breaking down the proposed IL algorithm and its incorporation into economic MPC. Finally, simulation results are presented and discussed in Section 4.

2. PROBLEM FORMULATION

In this section the ISTS to be considered in this paper is introduced, the ISTS control problem is defined, and the state space model for the ISTS is explained.

2.1 ISTS Description

The ISTS in question features a solar thermal collector (STC), a thermal storage tank (TST), and an auxiliary heat pump (HP) set up in a parallel fashion as seen in Fig. 1. The system has three loops, each containing a pump to circulate the fluid inside. In the STC loop the working fluid is glycol, while in the other loops it is water. A heat exchanger is used to transfer heat from the STC loop to the TST loop. The HP loop then supplies further heat to the TST as needed, with the HP containing a variable speed compressor which allows it to be controlled. Finally, the user hot water demand is taken from the top of the TST and replaced by relatively cold tap water at the bottom.

The system is subjected to two main disturbances: solar radiation and user load. Solar radiation is both the main energy source and a disturbance in the system. The total solar radiation flux at a given time of day determines the amount of energy available for collection. User load on the other hand is the central disturbance in the system and this paper's main topic of investigation. Many studies have determined that domestic hot water consumption varies over the course of a day, from day to day, from season to season, and is unique for each household (Knight et al., 2007, Edwards, Beausoleil-Morrison and Laperrière, 2015, George, Pearre and Swan, 2015). Despite these variations, there is still a repetitive nature to user load within each household which is exploited in this paper.

2.2 Problem Defnition

The control objectives for the ISTS are as follows:

(O1) Maintain the top layer temperature in the TST within a desired temperature range by regulating the compressor speed ratio of the HP.
(O2) Minimize HP operating costs while completing (O1).

The main challenge in achieving these objectives is the varying nature of hot water demand. The ideal controller must be able to efficiently perform the control task for multiple households, each featuring a unique load pattern that changes over time.

2.3 State Space Modelling

The ISTS control method, proposed in Section 3, utilizes the following discrete-time nonlinear state space model:

$$\mathbf{T}_{k+1} = f(\mathbf{T}_k, u_k, w_k). \tag{1}$$

Here $\mathbf{T} \in \mathbb{R}^n$ is the state vector consisting of the fluid temperatures at n different locations in the ISTS, u is the control input which is the HP compressor speed ratio, and w is the disturbance vector containing the solar radiation (s) $[\frac{W}{m^2}]$ and user hot water demand $(\dot{m})$ $[\frac{kg}{s}]$. Note that the output (y) of the model is the temperature at the top layer of the TST. This model was derived using the first law of thermodynamics as well as work completed in (Drück, 2006) and (Rostam, Nagamune and Grebenyuk, 2019).

3. CONTROLLER DESIGN

In order to achieve the control objectives given in Section 2.2, a control structure for the ISTS is proposed in Section 3.1, followed by an explanation of the IL method for load prediction in Section 3.2 and the resulting economic MPC formulation in Section 3.3.

3.1 Control Framework

In typical IL control, the error in a system's output relative to a reference trajectory is used to adjust the input for the next iteration (Bristow, Tharayil and Alleyne, 2006). In contrast, this paper uses load information from past iterations along with the error in past predictions to make load predictions for the next iteration. The block diagram for the control framework can be seen in Fig. 2. In this framework, previous load information is fed into the IL portion of the controller, which outputs an updated load trajectory prediction after each iteration for use in the MPC system model.

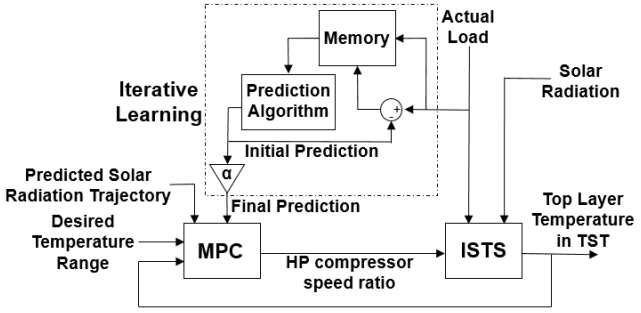

Fig. 2. Control framework of proposed method

Inside the IL portion of Fig. 2, the actual load over the course of an iteration is both stored in memory and compared to the latest initial prediction. The resulting difference between the initial prediction and the actual load at each time is also stored. At the end of each iteration, the information saved in memory is sent to the load prediction algorithm, which makes an initial prediction for the load trajectory of the next iteration. This initial prediction is then multiplied by a vector α, leading to the final load prediction, which serves as the updated load trajectory for the MPC. Similar to the initial load prediction, α is also determined after each iteration based on past information. Lastly, the initial prediction is fed back for comparison with the actual load of the next iteration and the IL process repeats. The specifics of this process are detailed further in Section 3.2.

3.2 Iterative Learning

In order to define a load trajectory prediction algorithm, some notation is first introduced:

$$W_g^{(i)} := \left[\, \dot{m}_1,\, \dot{m}_2,\, \ldots,\, \dot{m}_{k_f} \right]_g^{(i)}. \tag{2}$$

Here $W_g^{(i)}$ contains k_f discrete load values that represent the load trajectory for iteration i of group g. Each iteration represents one day, and days that are likely to have similar hot water demand profiles are grouped together. The specific grouping of days used in this paper is detailed in Section 4.1.

The following iterative algorithm for initial load trajectory prediction is then proposed:

$$\hat{W}_g^{(i+1)} = \frac{1}{\sum_{d=1}^{D} \rho_d} \sum_{d=1}^{D} \rho_d W_g^{(i+1-d)}, \tag{3}$$

where $\hat{W}$ designates the prediction of W. In this algorithm the initial load trajectory prediction for iteration $i+1$ of group g is taken as a weighted average of the load trajectories for the past D iterations of group g, with ρ_d being a weighting factor used to put more emphasis on recent information. As seen in Fig. 2, this initial prediction is compared with the actual load after each iteration and the resulting error is considered in the final load trajectory prediction algorithm:

$$\hat{\boldsymbol{W}}_g^{(i+1)} = \left[\, \hat{\dot{m}}_1,\, \hat{\dot{m}}_2,\, \ldots,\, \hat{\dot{m}}_{k_f} \right] = \alpha^{(i+1)} \odot \hat{W}_g^{(i+1)}, \tag{4}$$

where

$$\alpha^{(i)} := \mathbf{1} + \frac{1}{D_\alpha} \sum_{d=1}^{D_\alpha} E^{(i-d)} \oslash \hat{W}^{(i-d)}. \tag{5}$$

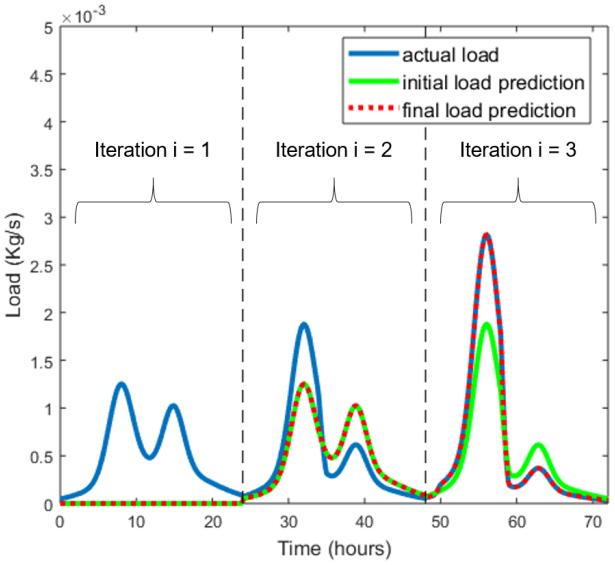

Fig. 3. Demonstration of IL prediction algorithm

Here $\odot$ and $\oslash$ denote elementwise multiplication and division, respectively, $E^{(i)} := W^{(i)} - \hat{W}^{(i)}$ is a vector of the error in the initial hot water demand prediction for iteration i, $\mathbf{1}$ is a vector of ones, and D_α is the number of past iterations to consider. As a whole, $\alpha^{(i)}$ is a vector representing the average percentage error in the load prediction at each time over the past D_α iterations regardless of group. It is used to account for trends in the load data that lead to consistent errors in initial load predictions and as such the group g of a given iteration is not considered in (5) since load trends tend to exist across all days (George, Pearre and Swan, 2015).

The functionality of the proposed algorithm is depicted in Fig. 3. In this figure, an arbitrary load trajectory that varies steadily over time is used for demonstration purposes. All days are considered to be in the same group and values of $D = 1$ and $D_\alpha = 1$ are implemented in (3) and (5). During the first iteration, previous load data is stored in memory and used to make load predictions for iteration $i = 2$. At this point, the initial and final load predictions are identical as there is not yet any information available on the prediction error of past iterations. After the second iteration, the error in the initial prediction can then be calculated and used to adjust the final prediction for iteration $i = 3$. Since a steadily varying load trajectory is used, this final prediction matches the actual load trajectory for iteration $i = 3$ perfectly while the initial prediction once again lags behind the trend.

3.3 Economic MPC

The economic model predictive controller for the ISTS is defined as

$$\min_{\substack{\{u_{k+j|k} \in \mathcal{U}\}_{j=1}^{N_p}, \\ \{(\gamma_j, \bar{\gamma}_j)\}_{j=1}^{N_p}}} \sum_{j=1}^{N_p} \mathbb{J}(\mathbf{T}_{k+j|k}, u_{k+j|k}, \underline{\gamma}_j, \bar{\gamma}_j, k)$$
$$\text{s.t.} \begin{cases} \mathbf{T}_{k+j+1|k} = f(\mathbf{T}_{k+j|k}, u_{k+j|k}, \hat{w}_{k+j|k}) \\ \underline{T} - \underline{\gamma}_j \le y_{k+j|k} \le \bar{T} + \bar{\gamma}_j \end{cases}. \tag{6}$$

Here N_p is the prediction horizon, $\underline{T}$ and $\bar{T}$ respectively represent the lower and upper boundaries of the desired temperature range, and the notation $v_{k+j|k}$ indicates the value of vector v at time $k+j$ when calculated at time k. In particular $\hat{w}_{k+j|k} = \begin{bmatrix} s_{k+j} \\ \hat{m}_{k+j} \end{bmatrix}$ indicates the disturbance prediction at time k for time $k+j$. The solar radiation portion of this prediction is simply obtained from the average solar radiation profile presented in Section 4.1, while the load trajectory portion is provided by the IL prediction algorithm in (4). Further, the control input for the system is constrained to $\mathcal{U} := [0, 1]$ due to compressor speed limitations, with zero relating to the HP being turned off and one relating to the HP functioning at full heating capacity. Lastly, to maintain the output temperature within the desired range while allowing slight variations to avoid an infeasible optimization problem, soft constraints are applied with the slack variables $\bar{\gamma}_j$ and $\underline{\gamma}_j$.

The cost function $\mathbb{J}$ consists of two terms,

$$\mathbb{J}(\mathbf{T}, u, \underline{\gamma}, \bar{\gamma}, k) \triangleq \mathbb{J}_{\text{EC}}(\mathbf{T}, u, k) + \mathbb{J}_{\text{CV}}(\underline{\gamma}, \bar{\gamma}). \tag{7}$$

The first term represents the economic cost of operating the HP and corresponds to (O2) while the second term corresponds to (O1) by penalizing temperature constraint violations in the top layer of the TST. The second term is detailed further as

$$\mathbb{J}_{CV}(\underline{\gamma}, \bar{\gamma}) \triangleq \underline{\eta}\underline{\gamma}^2 + \bar{\eta}\bar{\gamma}^2, \tag{8}$$

where $\underline{\eta}$ and $\bar{\eta}$ can be tuned to increase or decrease the controller's emphasis on preventing constraint violations.

Note that in the context of this paper (6) is solved using sequential quadratic programming.

4. SIMULATION

In order to verify the functionality of the proposed IL approach to load prediction, three separate simulations were carried out in Matlab. The simulations compare the following controllers:

(IL) proposed IL approach to economic MPC
(P) economic MPC with perfect load information
(A1) economic MPC that uses the average load profile to make load predictions
(A2) same as (A1) but with a shorter prediction horizon
(PI) proportional-integral controller

(P) produces the unrealistically optimal result while (A1) represents a method commonly used in previous literature (Rostam, Nagamune and Grebenyuk, 2019). (A2), with a shorter prediction horizon than (A1), was then included to examine robustness against inaccurate output predictions, since both (A1) and (A2) will have poor load information. Finally, (PI) acts as a baseline controller.

The specific parameters used in the simulation are first outlined in Section 4.1, followed by the simulation results themselves in Section 4.2.

4.1 Simulation Settings

Temperature Range: The desired temperature range of the top layer of the TST in the ISTS is between 60°C and 75°C, which are based on the building code for domestic hot water in Canada.

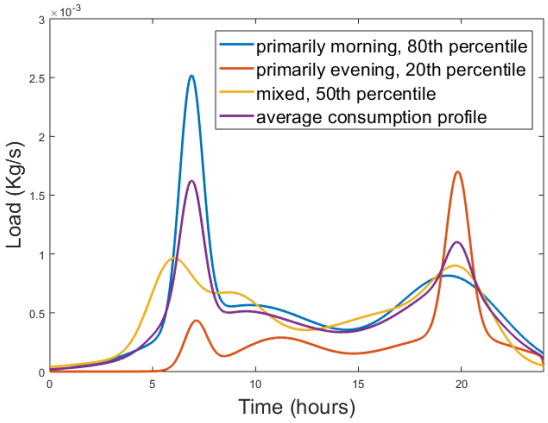

Fig. 4. Hot water demand profiles for use in simulation

State Space Model: A lumped approximation is used for the ISTS featuring seven states, with the state locations denoted by the temperature sensors in Fig. 1.

User Load: Data from (George, Pearre and Swan, 2015) was used to develop three load profiles, representative of three separate households and displayed in Fig. 4. These profiles are the most prevalent in the data, with the primarily morning profile (A) being the most common, followed by the primarily evening profile (B), and finally the mixed profile (C). Note that the average load profile across all featured households (D) is also shown in Fig. 4 and is used for prediction in (A1) and (A2).

In order to test the effectiveness of (IL), the developed profiles should vary according to daily and seasonal trends. The data demonstrates that different loads can be expected on different days, as depicted in Table 1. Further, while load trajectory shapes remain similar within individual households on Monday through Saturday, load trajectories tend to shift on Sunday, with morning peaks occurring 3 hours later. Additionally, daily domestic loads shift with the seasons as more hot water is consumed in colder months. Specifically, 2.8% more demand than average is expected in the winter, while in the summer demand falls by 9.6% (George, Pearre and Swan, 2015).

Table 1. Daily hot water consumption relative to average

Day	M	T	W	Th	F	Sa	Su
Deviation (%)	0	0	-1.45	-2.9	-8.7	1.45	11.59

For a realistic representation of various households, different consumption levels should also be represented. With that in mind, as seen in Fig. 4, the primarily morning profile is associated with hot water demand in the 80th percentile at 220 kg/day, the primarily evening household is assumed to use hot water in the 20th percentile at 93 kg/day, and the mixed profile household consumes in the 50th percentile at 172 kg/day.

For the three simulations, four weeks' worth of daily load profiles were created for each of the three households. These profiles vary in day-to-day consumption levels and trajectories based on the trends explained above. They also gradually go from mid-winter consumption levels at the start of the four weeks to mid-summer levels at the

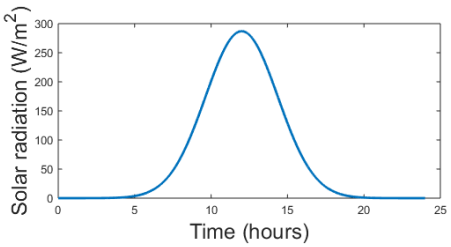

Fig. 5. Solar radiation profile for Vancouver, Canada on Jan 1st

end of the four weeks so as to demonstrate the proposed IL method's ability to track these changes.

Solar Radiation: The daily solar radiation profile used in this paper is based on a mathematical model presented in (Khatib and Elmenreich, 2016), and displayed in Fig. 5. Note that a constant daily profile is used since varying solar radiation is not the main focus of this paper.

Cost of Electricity: The operating cost of the HP at a given time is a function of the cost of electricity at that time. Canadian electrical time-of-use price periods are adopted in the simulations and are depicted in Table 2.

Table 2. Time-of-use electrical price periods

Time of day (hours)	0-7	7-11	11-17	17-19	19-24
Cost (¢/kWh)	6.5	9.4	13.4	9.4	6.5

Controller Settings: The baseline PI controller uses the following rule to set the control input

$$u(t) = \begin{cases} k_p e(t) + k_i \int e(t)dt, & y \leq \underline{T} \\ 0, & \text{otherwise} \end{cases}, \tag{9}$$

where

$$e(t) := \underline{T} - y(t). \tag{10}$$

The coefficients k_p and k_i are tuning parameters that specify the aggressiveness of the controller, and the input is maintained between 0 and 1 using a saturation block. For the simulations, k_p and k_i were tuned through trial and error and are set to 150 and 0.001, respectively.

For both (IL) and (P) the prediction horizon is set as $N_p = 12$ hours, which gives them enough time to adjust to upcoming disturbances. Similarly (A1) uses $N_p = 12$ hours, while (A2) uses $N_p = 2$ hours. Further, all economic MPC controllers use $\eta = \bar{\eta} = 100$. Additionally, since hot water demand profiles vary every day, as seen in Table 1, days are divided into seven groupings, with a group g for each day of the week.

Lastly, the averaging parameters for the IL portion of (IL) are chosen as $D = 1$ and $D_\alpha = 7$ and the IL method utilizes the designed PI controller for the first week of operation. After a week, enough load information is stored for predictions to be made and the MPC technique is reinstated. This load information is provided by a flowmeter at 1 minute intervals.

4.2 Simulation Results

Complete results of the simulations are summarized in Table 3, where the important performance metrics to consider are cost, average constraint violation (ACV), and average daily maximum constraint violation (AMCV). Output temperature and control input plots for the Tuesday of the second week of simulations for load profile (B) are then displayed in Fig. 6(a) and Fig. 6(b) respectively.

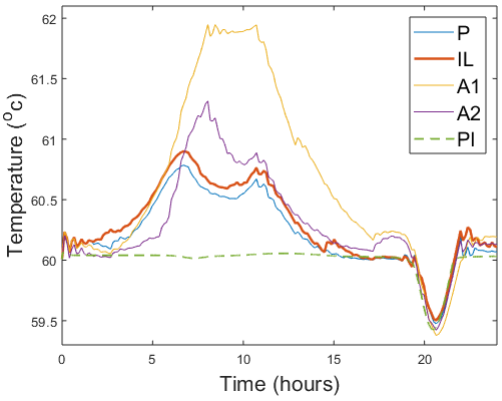

(a) Top layer temperature of the TST

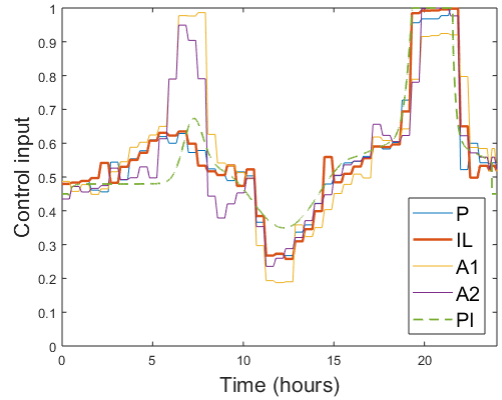

(b) Compressor speed ratio inside HP

Fig. 6. Performance of various controllers on the Tuesday of the second week of simulations for load profile (B)

Examining Table 3, it is clear that (IL) performed nearly as well as (P), while outperforming the other control strategies in every category. It is also interesting to note that (A2) outperformed (A1) in all cases, indicating that a shorter prediction horizon may be beneficial in the presence of prediction error. More work is needed to draw any meanigful conclusions from this observation though.

By inspecting Fig. 6, it is apparent that (IL) was able to manage the ISTS output temperature quite effectively while limiting cost. Looking specifically at Fig. 6(a), the need for accurate load prediction is revealed. In this plot, (A1) and (A2) drastically overheat the system between hours 5 and 15 in anticipation of a larger load than there is. Since (IL) is able to predict the load trajectories with greater accuracy, it avoids this problem. Now observing Fig. 6(b), it becomes clear why (IL) outperforms (PI). In the first 7 hours, (IL) heats the system more than required so as to take advantage of off-peak energy pricing. This then allows (IL) to reduce energy usage between hours 7 and 15 compared to (PI), when energy is more expensive.

Table 3. Performance results of examined controllers

Load Profile (A)					
Controller	P	IL	A1	A2	PI
Avg daily cost ($)	4.54	4.56	4.62	4.58	4.65
Deviation (%)	-	0.44	1.76	0.88	2.42
ACV (°C)	0.07	0.09	0.13	0.09	0.11
Deviation (%)	-	28.57	85.71	28.57	57.14
AMCV (°C)	0.92	1.02	1.27	1.19	1.31
Deviation (%)	-	10.87	38.04	29.35	42.39
Load Profile (B)					
Controller	P	IL	A1	A2	PI
Avg daily cost ($)	3.50	3.51	3.66	3.55	3.55
Deviation (%)	-	0.29	4.57	1.43	1.43
ACV (°C)	0.02	0.02	0.04	0.03	0.03
Deviation (%)	-	0.00	100.00	50.00	50.00
AMCV (°C)	0.50	0.50	0.59	0.57	0.57
Deviation (%)	-	0.00	18.00	14.00	14.00
Load Profile (C)					
Controller	P	IL	A1	A2	PI
Avg daily cost ($)	4.30	4.31	4.42	4.33	4.38
Deviation (%)	-	0.23	2.79	0.70	1.86
ACV (°C)	0.00	0.00	0.01	0.01	0.00
Deviation (%)	-	0.00	∞	∞	0.00
AMCV (°C)	0.01	0.01	0.09	0.08	0.01
Deviation (%)	-	0.00	800.00	700.00	0.00

5. CONCLUSION

A new iterative learning approach was proposed for disturbance prediction in economic model predictive control and applied to a domestic integrated solar thermal system. Simulations were developed based on real world hot water demand data, and the performance of the proposed method relative to existing control options demonstrated its effectiveness. In future research, the robustness of the proposed method will be examined by testing it with real life domestic hot water consumption data from individual households. The notion of adjusting the MPC prediction horizon relative to variance in the collected load data will also be investigated since shorter prediction horizons tend to lead to more robust controllers in the presence of prediction error, as evidenced in this paper. Further, increasingly intelligent iterative load prediction algorithms involving machine learning techniques for pattern recognition will be examined.

REFERENCES

Aguilar, C., White, D. and Ryan, D. (2005). *Domestic Water Heating and Water Heater Energy Consumption in Canada*. Calgary: Canadian Building Energy End-Use Data and Analysis Center.

Armstrong, M., Swinton, M., Ribberink, H., Beausoleil-Morrison, I. and Millette, J. (2009). Synthetically derived profiles for representing occupant-driven electric loads in Canadian housing. *Journal of Building Performance Simulation*, 2(1), pp. 15–30.

Box, G., Jenkins, G., Reinsel, G. and Ljung, G. (2015). *Time Series Analysis: Forecasting and Control*. 5th ed. Wiley.

Bristow, D., Tharayil, M. and Alleyne, A. (2006). A survey of iterative learning control. *IEEE Control Systems Magazine*, 26(3), pp. 96–114.

Crabtree, G. and Lewis, N. (2007). Solar energy conversion. *Physics Today*, 60(3), pp. 37–42.

Drück, H. (2006). *Multiport store - model for TRNSYS*. Institut für Thermodynamik und Wärmetechnik (ITW), Universität Stuttgart.

Edwards, S., Beausoleil-Morrison, I. and Laperrière, A. (2015). Representative hot water draw profiles at high temporal resolution for simulating the performance of solar thermal systems. *Solar Energy*, 111, pp. 43–52.

Energy Saving Trust (2008). *Measurement of domestic hot water consumption in dwellings*. UK Department of Energy and Climate Change.

Fuentes, E., Arce, L. and Salom, J. (2018). A review of domestic hot water consumption profiles for application in systems and buildings energy performance analysis. *Renewable and Sustainable Energy Reviews*, 81, pp. 1530–1547.

Gelazanskas, L. and Gamage, K. (2015). Forecasting hot water consumption in residential houses. *Energies*, 8, pp. 12702–12717.

George, D., Pearre, N. and Swan, L. (2015). High resolution measured domestic hot water consumption of Canadian homes. *Energy and Buildings*, 109, pp. 304–315.

Godina, R., Rodrigues, E., Pouresmaeil, E., Matias, J. and Catalão, J. (2018). Model predictive control home energy management and optimization strategy with demand response. *Applied Sciences*, 8(3), pp. 408–426.

Khatib, T. and Elmenreich, W. (2016). *Modeling of photovoltaic systems using MATLAB*. Wiley.

Kircher, K. and Zhang, K. (2015). Model predictive control of thermal storage for demand response. In: *IEEE American Control Conference (ACC)*, pp. 956—961

Knight, I., Kreutzer, N., Manning, M., Swinton, M. and Ribberink, H. (2007). *European and Canadian non-HVAC electric and DHW load profiles for use in simulating the performance of residential cogeneration systems*. International Energy Agency.

Lee, K., Chin, I., Lee, H. and Lee, J. (2004). Model predictive control technique combined with iterative learning for batch processes. *AIChE Journal*, 45(10), pp. 2175–2187.

Lu, P., Chen, J. and Xie, L. (2018). Iterative learning control based economic optimization for batch processes using helpful disturbance information. *Industrial & Engineering Chemistry Research*, 57(10), pp. 3717–3731.

Ma, Y., Kelman, A., Daly, A. and Borrelli, F. (2012). Predictive control for energy efficient buildings with thermal storage: modeling, simulation, and experiments. *IEEE Control Systems Magazine*, 32(1), pp. 44–64.

Mohtasham, J. (2015). Review Article-Renewable Energies. *Energy Procedia*, 74, pp. 1289–1297.

Rosolia, U. and Borrelli, F. (2018). Learning model predictive control for iterative tasks. A data-driven control framework. *IEEE Transactions on Automatic Control*, 63(7), pp. 1883–1896.

Rostam, M., Nagamune, R. and Grebenyuk, V. (2019). Analysis of economic model predictive control parameter selection in an integrated solar thermal system. In: *IEEE Conference on Control Technology and Applications*, pp. 209–214.

Weeratunge, H., Narsilio, G., de Hoog, J., Dunstall, S. and Halgamuge, S. (2018). Model predictive control for a solar assisted ground source heat pump system. *Energy*, 152, pp. 974–984.